Desalination and Water Treatment
www.deswater.com

doi: 10.5004/dwt.2018.23095

136 (2018) 273–281
December

Elimination and absorption of butachlor from water aqueous containing herbicide by modified magnetic graphene oxide

Soha Nozhat[a], Amir Hessam Hassani[a,*], Homayon Ahmad Panahi[b], Elham Moniri[c], Masoud Monavari[a]

[a]*Department of Natural Resources and Environment, Science and Research Branch, Islamic Azad University, Tehran, Iran; emails: ahhassani@srbiau.ac.ir (A.H. Hassani), nozhat.s@gmail.com (S. Nozhat), m-monavari@srbiau.ac.ir (M. Monavari)*
[b]*Department of Chemistry, Central Tehran Branch, Islamic Azad University, Tehran, Iran; email: h.ahmadpanahi@iauctb.ac.ir*
[c]*Department of Chemistry, Varamin-Pishva Branch, Islamic Azad University, Varamin, Iran; email: moniri30003000@yahoo.com*

Received 19 April 2018; Accepted 2 September 2018

ABSTRACT

The pollution of agricultural wastewater by herbicides has become a major environmental challenge. To lessen the impact of this phenomenon, nanomagnetic graphene oxide was used as a novel adsorbent. This synthesized adsorbent was immobilized with a thermosensitive polymer (TSP) and modified with an organic dendrimer (methyl methacrylate and ethylenediamine). The use of this novel-synthesized substance for removing pollutants from an aqueous solution was studied. The composition and morphology of GO/Fe_3O_4 grafted with TSP and dendrimer (GO/Fe_3O_4/TSP/Den) were characterized by Fourier-transform infrared spectroscopy, transmission electron microscopy, scanning electron microscopy, energy-dispersive X-ray spectroscopy, X-ray diffraction, vibrating-sample magnetometer, and thermogravimetric analysis. Parameters such as solution pH, contact time, adsorption isotherm, and reusability were evaluated. The results indicated that GO/Fe_3O_4/TSP/Den had efficient adsorption ability at a pH value of 5, a time period of 45 min, 1 mg L^{-1} concentration of the pollutant, a temperature of 37°C, and a dose of 3 g L^{-1} of adsorbent. The adsorption capacity remained at 93.3% after 10 repetitions. The butachlor adsorption process follows pseudo-second-order kinetics equations and the Langmuir adsorption model. Moreover, the thermodynamic process was investigated for indicating the spontaneous and endothermic process of adsorption in nature. Eventually, the results demonstrated that GO/Fe_3O_4/TSP/Den had an impressive adsorption capability to eliminate butachlor in wastewater and it can be quickly removed from water.

Keywords: Graphene oxide; Magnetic particles; Dendrimer; Butachlor

1. Introduction

Increasing water consumption and subsequent water scarcity, which have been exacerbated by water pollution, has made water supply a major concern for the international community [1]. Water quality is decreasing every day due to the arrival of fertilizers and insecticides used in agricultural affairs. Owing to their high consumption and concentration, pesticides could enter the environment via industrial wastewater and agricultural drainage [2]. Toxic substances used in agriculture can penetrate water resources through washing or irrigation at the sites of consumption [3]. Chloroacetanilide herbicides (e.g., acetochlor, metolachlor, and butachlor [BUT]) are the main chemicals used in agricultural activities all over the world, especially in rice fields [4]. Nowadays, the large-scale usage of BUT is prevalent on the surface water and groundwater, which leads to the disruption of the environment and ecosystems. Many

* Corresponding author.

researchers have warned that BUT, in aquatic ecosystems, is a major environmental risk for microorganisms such as algae and fish. BUT may enter the surrounding water after drainage, irrigation, and through agricultural runoff, leading to the risk of water pollution and damage to the health of aquatic ecosystems [5]. Therefore, eliminating the use of BUT is urgent for safeguarding human health and environmental improvement. Graphene oxide (GO) has a high specific surface and several functional groups containing oxygen (carboxyl, hydroxyl, and epoxy), which are attached to its layers with covalent bonds, leading to a negative charge level [6–11]. For this reason, GO is typically used as an adsorbent and dissipates into the sample solution for adsorption, centrifugation, or filtration; it is then separated or recovered with dispersion. Magnetic nanoparticles (Fe_3O_4) are extensively used in environmental applications because they have exclusive magnetic properties and lead to rapid separation of molecules from the sample by using an external magnetic field [12–17]. In the same way, magnetic particles located on graphene and magnetic particle–graphene composite responded to a magnet that could realize the recovery and separation of graphene from dispersion quickly and successfully. GO is used for preventing the accumulation of pulverized Fe_3O_4. Dendrimer is a polymer with various industrial applications [18–21]. Dendrimers comprise a family of three-dimensional polymers on the nanoscale. Dendrimers can transport guest molecules to receptors on their surface or encapsulated within the cavities contained in the branches [22]. Dendrimers grafted on GO/Fe_3O_4 prevent the oxidation of Fe_3O_4 nanoparticles. By introducing a dendrimer that is grafted on the carbon base, the adsorption capacity of the nanohybrid can be controlled.

Liu et al. [23] reported that herbicide 2,4-dichlorophenoxyacetic (2,4-D) could be efficiently removed by reduced GO and $CuInS_2$ co-decorated TiO_2 nanotubes. The photodegradation rate is 96.2% [23]. Mahmoodi et al. [12] reported that the degradation of BUT in an aqueous solution by nanophotocatalysis using immobilized TiO_2 was an effective method for removing BUT from contaminated water. Tang et al. [24] investigated the removal utility of herbicides (2,4-D) from water by the magnetic TiO_2-graphene composite. In this study, it was found that after the use of the adsorbent eight times to remove 2,4-D, 97.7% of the adsorbent could be retained [24].

In this study, synthesized magnetic GO grafted with thermosensitive polymer (TSP) and dendrimer "GO/Fe_3O_4/TSP/Den" nanocomposite was used as a newly designed adsorbent for BUT elimination. The application of the synthesized sorbent by increasing the adsorbent capacity and changing it to a reusable adsorbent was investigated by analyzing parameters such as pH, contact time, the initial concentration of BUT, the amount of adsorbent, and adsorption temperature.

2. Materials and methods

2.1. Chemicals

BUT (95% purity) was purchased from Arya Chemistry Co. (Sistan and Baluchestan Province, Iran). The chemical structure of BUT is depicted in Fig. 1. BUT ($C_{17}H_{26}NO_2$), *N*-butoxymethyl-2-chloro-2',6'-diethylacetanilide, is a systemic and selective herbicide used to control weeds in rice fields [12,25].

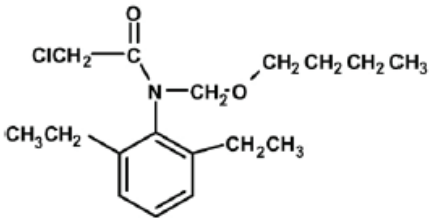

Fig. 1. The chemical structure of Butachlor.

Iron (II) chloride, iron (III) chloride, dimethylformamide (DMF), 1,4-dioxane, petroleum ether, *N*-vinyl caprolactam, and azobisisobutyronitrile (AIBN) were supplied by Sigma-Aldrich (Munich, Germany) and methanol, ethanol, methyl methacrylate, ethylenediamine (EDA) (Merck & Co., Darmstadt, Germany), allylamine (Merck & Co., Hohenbrunn, Germany), and others were purchased from Merck (Frankfurt, Germany). GO was purchased from Pishgaman Nano Arya Co., Ltd., Mashhad, Iran.

2.2. Instruments

Transmission electron microscopy (TEM) images of "GO/Fe_3O_4/TSP/Den" were recorded on a Philips EM 208 (FEI Company, Eindhoven, Netherlands), and Fourier-transform infrared spectroscopy (FTIR) spectra were obtained using an FTIR (Nexus 870 FTIR, Thermo Nicolet, USA). Magnetic property was performed on a vibrating-sample magnetometer (Lakeshore Cryotronics 7400, Ohio, USA) at room temperature, and the crystal phases were recognized by X-ray diffraction (XRD) patterns with Seifert-XRD 3003 PTS. Scanning electron microscopy (SEM) images were procured by using a SEM microscope (Vega Model, TESCAN USA Inc.), and the adsorbent chemical compounds were found by energy-dispersive X-ray (EDX) spectroscopy performing in SEM. The amount of EDA and methyl methacrylate dendrite bounding on GO/Fe_3O_4 was estimated by thermogravimetric analysis (TGA) by using Nietzsche TGA 209 F1 with a heating rate of 10°C min^{-1} at the temperature of 600°C under air.

2.3. Preparation of "GO/Fe_3O_4/TSP/Den"

2.3.1. Preparation of GO/Fe_3O_4

First, $FeCl_3.6H_2O$ (6.8 g), $FeCl_2.4H_2O$ (3.5 g), GO (1.0 g), and deionized water (250 mL) were mixed in an Erlenmeyer flask in an ultrasonic bath at 80°C for 30 min. Besides, 10 mL of 32% ammonia was added gradually over 15 min in reflux conditions at 80°C and was constantly stirred into the previous contents. In addition, the solution was stirred at room temperature for 24 h. Finally, the produced nanocomposite was separated by a magnetic field by applying a 1.4 Tesla magnifier and dried in an oven.

2.3.2. Preparation of "GO/Fe_3O_4/TSP/Den"

The dendrimerization method was used to modify magnetic GO. In this research, the following steps were performed:

- Step 1: First, 50 mL solution of 1,4-dioxane and petroleum ether along with 0.5 g of cyanuric chloride were added to GO/Fe_3O_4 at room temperature and stirred for 3 d. After that, the mixture was washed with dioxane and petroleum ether.
- Step 2: 20 mL of DMF and 8 mL of allylamine were added to GO/Fe_3O_4 at 50°C and stirred mechanically (1,000 rpm) for 1 d. The obtained nanoparticles were washed with DMF.
- Step 3: 20 mL of ethanol, 1 g of *N*-vinyl caprolactam, 10 mL of allylamine, and nano of previous stage were mixed for 10 min under an N_2 atmosphere. Then 1 g of AIBN was added, and the mixture was refluxed in a nitrogen atmosphere for 7 h at 60°C–70°C. Last, it was washed with 20 mL of ethanol. In this step, "GO/Fe_3O_4/TSP" was produced.
- Step 4: It involved a two-step bonding of the 10 branches to the previously synthesized nanoparticles. First, 150 mL of methanol and 15 mL of methyl methacrylate were added into "GO/Fe_3O_4/TSP" under an N_2 atmosphere at 50°C for 24 h. Next, 150 mL of methanol and 30 mL of EDA were refluxed at 50°C for 24 h. These two steps were repeated 10 times. In this step, "GO/Fe_3O_4/TSP/Den" was synthesized.

Subsequently, the synthesized adsorbent was washed with methanol, centrifuged, separated by a super magnet, and dried in the oven at low temperature (Fig. 2).

As shown in Fig. 3, in a typical state, the adsorbent is dispersed in an aqueous solution after a few minutes, while this magnetic adsorbent is accumulated within a few minutes by an external magnet and a clear solution is obtained that can be well measured for separation efficiency.

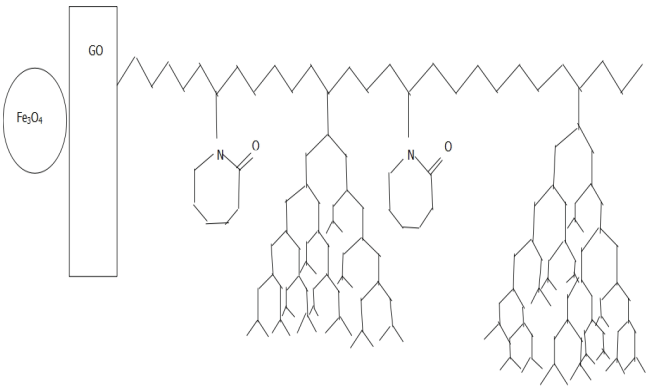

Fig. 2. The schematic of "GO/Fe_3O_4/TSP/Den".

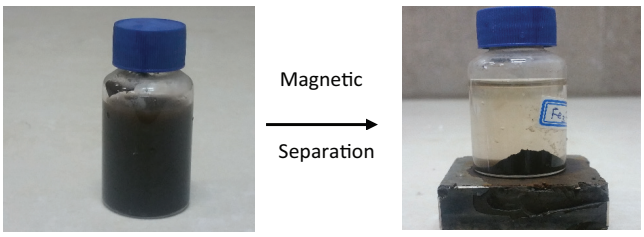

Fig. 3. Photographs of magnetic nanoadsorbent (a) without and (b) with external magnetic field.

2.4. Adsorption and removal of BUT with "GO/Fe_3O_4/TSP/Den"

First of all, a sample of BUT solution was studied with spectrophotometer UV-Vis (DR5000, Hach Company, Colorado, USA) to select operational λ (212 nm). The removal of BUT from aqueous solutions by "GO/Fe_3O_4/TSP/Den" sorbents was accomplished with the experimental methods. The standard stock solution (100 mg L^{-1}) of BUT was prepared in ethanol-distilled water (20.80) and stored at 0°C. All the experimental samples of BUT had a 10 mg L^{-1} concentration and were prepared daily by diluting the stock solutions. The adsorption experiments were carried out in beakers at room temperature. Initially, 3 g L^{-1} of "GO/Fe_3O_4/TSP/Den" sorbents were rinsed and dispersed into 10 mL of experimental samples. Furthermore, the mixture was shaken for 30 min. In the end, a strong magnet was placed at the bottom of the beaker and the sorbents were separated from the solution. After around 30 s, the solution became clear and overflowed easily. Last of all, in this process and for all the remaining steps, the final supernatant of BUT was identified by a UV-Vis spectrophotometer at 212 nm.

The removal percentage (E) of "GO/Fe_3O_4/TSP/Den" on BUT is measured as follows:

$$E\,(\%) = \frac{C_0 - C_e}{C_0} \times 100 \tag{1}$$

Here, C_0 and C_e are the initial and final equilibrium concentrations of BUT (mg L^{-1}) in the aqueous solution, respectively [26].

2.4.1. Adsorption kinetics

First of all, "GO/Fe_3O_4/TSP/Den" (3 g L^{-1}) was added to the BUT solution (10 mL, 10 mg L^{-1}). The combination was vibrated at 500 rpm at 25°C. Then, the adsorbent was adsorbed by a super magnet and the supernatant was filtered by syringe filter.

2.4.2. Adsorption isotherm

"GO/Fe_3O_4/TSP/Den" (3 g L^{-1}) was added to the BUT solution (10 mg L^{-1}) in the range of 1–50 mg L^{-1} concentration. The mixture was shaken at 550 rpm at 25°C for 45 min. Then, it was magnified and the supernatant was filtered by syringe filter.

2.4.3. Adsorption thermodynamics

To determine the effect of temperature on BUT adsorption, thermodynamic experiments were also conducted at 25°C, 30°C, and 40°C.

2.4.4. Reusability of "GO/Fe_3O_4/TSP/Den"

"GO/Fe_3O_4/TSP/Den" (0.04 g) was placed in a conical flask containing BUT solution (10 mL, 10 mg L^{-1}), and the mixture was shaken in a temperature-controlled oscillator at 25°C for 5 min. The mixture was separated by using a magnet and the final concentration of BUT was determined. "GO/Fe_3O_4/TSP/Den" was recycled by washing.

2.5. Preparation of real water sample

In order to investigate the application of this method on a real scale, it was used for the analysis of the BUT in agricultural wastewater that was gathered from an agricultural field of Doroudzan Dam, Fars, Iran. Then, three samples were provided under laboratory conditions (pH = 5, the amount of adsorbent was 0.1 g for 45 min, 5 mg L^{-1}, 10 mL). It was used for calculating the removal percentage of BUT by high-performance liquid chromatography (HPLC). Chromatographic determination of BUT was accomplished by KNAUER wavelength UV/Vis detector fixed to 212 nm and C18 (16 mm × 250 mm, 10 μL) column from Berlin, Germany. The infusion volume was 20 μL; the mobile phase was a blend of methanol and water (37:63 v/v) with a flow rate of 1.0 mL min^{-1}[27].

3. Results and discussion

3.1. Characterizations of "GO/Fe_3O_4/TSP/Den"

The FTIR spectrum of GO (Fig. 4(a)), GO/Fe_3O_4 (Fig. 4(b)), and GO/Fe_3O_4/TSP (Fig. 4(c)) showed the O–H, C=O, H–C–H, and C–O stretching vibration peaks at 3,421, 1,730, 1,462, and 1,100 cm^{-1}, respectively. These peaks (1,126 and 1,632 cm^{-1} belonging to C–O and C=O in the FTIR of GO) provide evidence of the existence of carboxyl and epoxy groups in GO. The O–H stretching vibration of the aliphatic group and Fe–O bands in GO/Fe_3O_4 and GO/Fe_3O_4/TSP structure was observed at 2,923 and 605 cm^{-1}, respectively. As shown, the peaks at 1,570 and 1,032 cm^{-1} are the N–H and Si–O bands in the FTIR of TSP. The peaks around 600 cm^{-1} have been linked to Fe–O and indicated the successful loading of Fe_3O_4 NP_s onto GO. In the FTIR spectrum of "GO/Fe_3O_4/TSP/Den" (Fig. 4(d)), the observed peaks at 1,042, 1,118, and 1,323 cm^{-1} are Si–O, C–O, and C–N bands, respectively. The 1,473 cm^{-1} peak is for the CH_2 group. The observed peak at 1,655 cm^{-1} pertains to O–H and 1,741 cm^{-1} accounts for C=O. The wide peak monitored at 3,471 cm^{-1} is related to the O–H bond. All the results confirm that "GO/Fe_3O_4/TSP/Den" has been well synthesized.

The XRD patterns of pure GO and GO/Fe_3O_4 samples are presented in Figs. 5(a) and (b). As noted in previous reports, usually, the natural graphite exposes a basal reflection (002) peak at 2θ = 26.6°. When the oxygen functionalities interact with the main plan of the graphite, after oxidation of the natural graphite, the 002 reflection peak moves to 2θ = 12.3°. From the XRD pattern of GO/Fe_3O_4 analysis, the main characteristic peaks of Fe_3O_4 and GO are located at 10.3°, 30.1°, 35.4°, 43.3°, 54.5°, 57.3°, and 62.8° illustrating that the product is composed of two phases, that is, Fe_3O_4 and GO.

The EDX spectrum of TSP (Fig. 6(a)) and "GO/Fe_3O_4/TSP/Den" (Fig. 6(b)) indicate that the elements of carbon, nitrogen, and oxygen were in TSP and "GO/Fe_3O_4/TSP/Den". The elements ratio of carbon, nitrogen, oxygen, and iron is 47.67%, 13.89%, 38.37%, 0.02%, and 0.04% in TSP, respectively. Otherwise, the respective ratios of these elements in "GO/Fe_3O_4/TSP/Den" are 53.84%, 16.08%, 30.01%, 0.03%, and 0.04%. It proves that dendrimer is successfully coated with the TSP nanoparticles. In fact, due to the presence of nitrogenous organic dendrimers on the adsorbent, the percentage of carbon and nitrogen has risen.

Fig. 7 illustrates the super magnetization curves of "GO/Fe_3O_4/TSP/Den" at room temperature. The maximum saturation of super magnetizations of "GO/Fe_3O_4/TSP/Den" is measured at 28.6 emu g^{-1}. According to Saber et al.'s [28] study, a saturation super magnetization of 16.3 emu g^{-1} is enough for magnetic separation from the solution with a magnet. This implies that sorbents can be easily dispersed into water solution, and the magnetic sorbent loaded with analyses can be isolated from the matrix conveniently by using an external magnet when necessary. Meanwhile, the external magnetic field is taken away, and these sorbents can redisperse rapidly.

The surface morphology of the TSP and "GO/Fe_3O_4/TSP/Den" was shown by SEM (Figs. 8(a) and (b)) and TEM (Fig. 8(c)). As shown, the magnetic particles are successfully

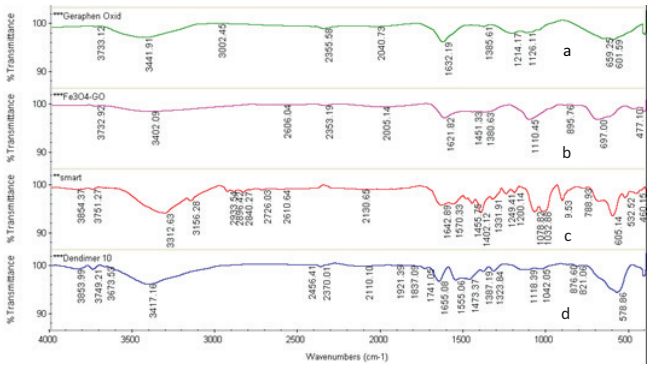

Fig. 4. FTIR of (a) GO, (b) GO/Fe_3O_4, (c) GO/Fe_3O_4/TSP, and (d) GO/Fe_3O_4/TSP/Den.

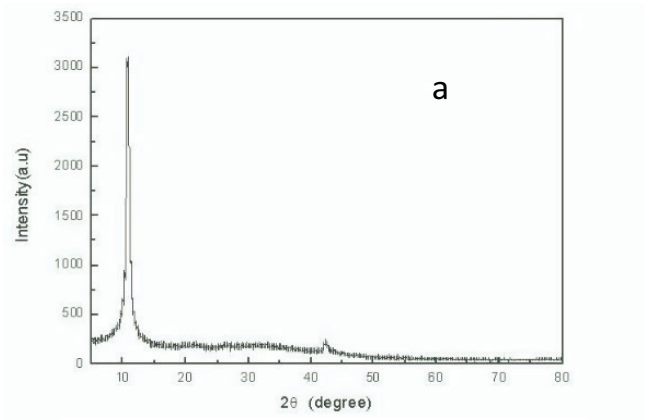

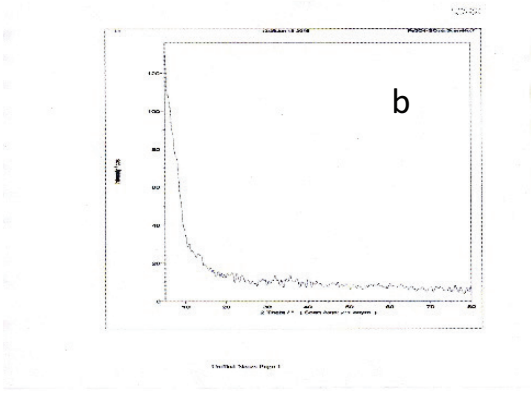

Fig. 5. XRD patterns of (a) GO and (b) GO/Fe_3O_4.

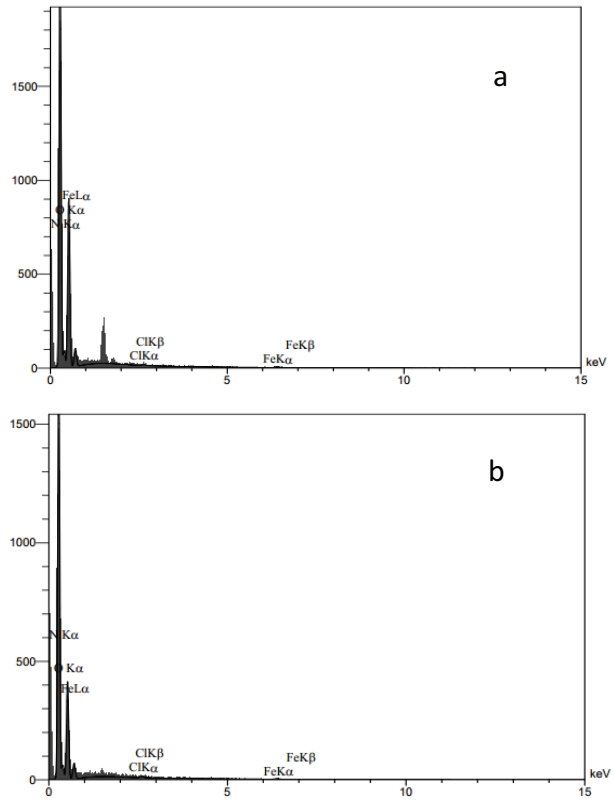

Fig. 6. EDX spectrum of (a) GO/Fe_3O_4/TSP and (b) GO/Fe_3O_4/TSP/Den.

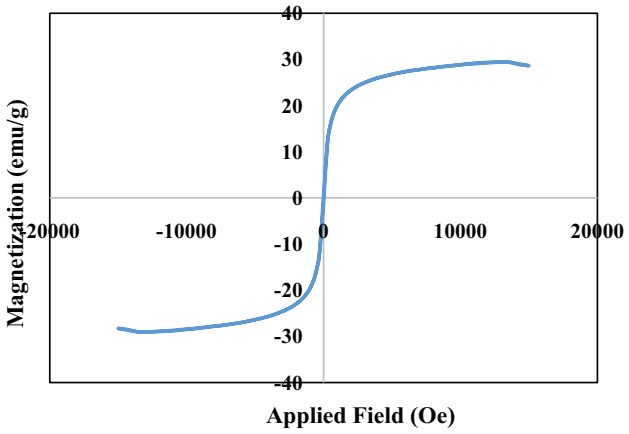

Fig. 7. Vibrating-sample magnetometer super magnetization curves of GO/Fe_3O_4/TSP/Den.

placed on GO. The sizes of synthesized Fe_3O_4 particles on GO surface are in the range of 40–60 nm.

TGA was employed for evaluating the amount of a sample mass measured over time as the temperature changes in the nanohybrid. The thermogram of TSP showed the first 1.38% mass loss (approximately 100°C), which is due to water solvent molecules adsorbed into the GO/Fe_3O_4 nanoparticles. 4.83% weight loss at 200°C is observed for removing dendrimers and 10% weight loss at 350°C to remove the grafted polymers (Figs. 9(a) and (b)).

Fig. 8. SEM images of (a) TSP and (b) GO/Fe_3O_4/TSP/Den and (c) TEM image of GO/Fe_3O_4/TSP/Den.

3.2. Effect of pH

The stock solution was made in the range of pH 3, 4, 5, 6, 7, and 8, to investigate the effect of initial pH on BUT adsorption. Fig. 10 shows that the optimum pH is 5. In acidic pH ranges (3–5), the removal productivity increased. On the other hand, in natural and alkaline pH ranges, the pH had an insignificant impact on removal productivity. Whenever the pH increased to 5, 99% of BUT was eliminated. BUT has a negative charge due to the carboxylic and phenolic groups in the pH range of 4–8. The charge of the adsorbent surface was positive due to the effect of the proton reaction in pH less than pH-isoelectric peaks (pI = 8), and hence a strong electrostatic bond between the adsorbent surface and BUT was established.

3.3. Adsorption kinetics

Two of the most important kinetic models for the study of the mechanism of adsorption kinetics are pseudo-first-order and pseudo-second-order kinetics, to evaluate the sorption kinetics.

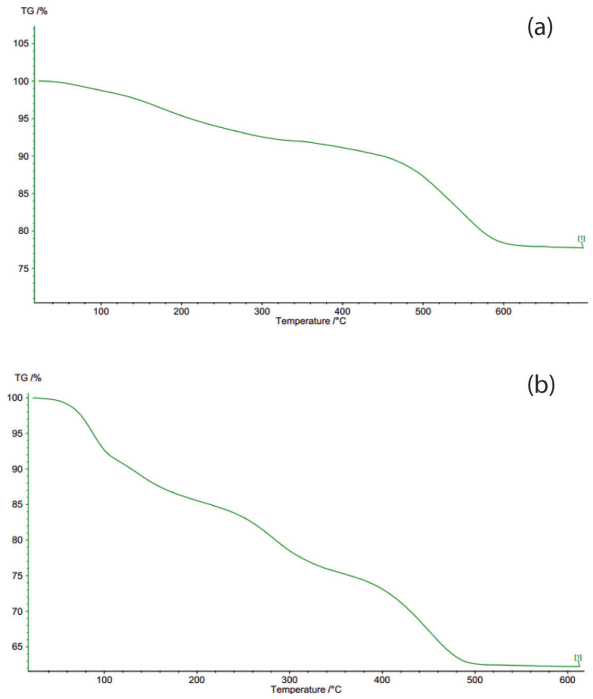

Fig. 9. TGA analysis of (a) TSP and (b) GO/Fe_3O_4/TSP/Den.

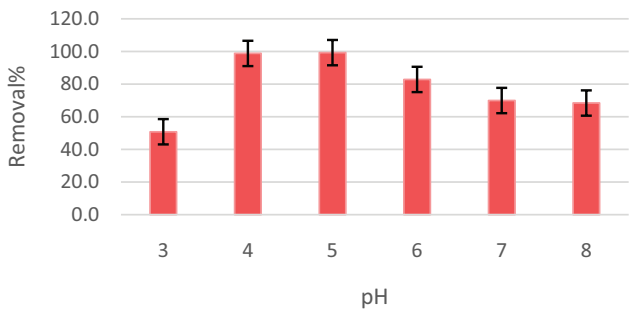

Fig. 10. The influence of initial pH on the removal of BUT.

It is necessary to introduce the correlation coefficient (R^2, close or equal to 1) to estimate the suitability of different models. A higher R^2 value indicates a more applicable kinetic model. The kinetic model is expressed by the following equation:

$$\ln(q_e - q_t) = \ln q_e - k_1 t \tag{2}$$

$$\frac{t}{q_t} = \frac{1}{k_{ad} q_e^2} + \frac{1}{q_e} t \tag{3}$$

Here, k_{ad} (g mg^{-1} min^{-1}) is the rate constant of adsorption, q_e (mg g^{-1}) is the equilibrium adsorption capacity, and q_t (mg g^{-1}) is the amount was adsorbed at the time.

The intraparticle diffusion rate is expressed according to the following equation:

$$q_t = k_i t^{0.5} \tag{4}$$

Here, k_i is the intraparticle diffusion rate constant (mg/(g min$^{0.5}$)), and the value of k_i can be calculated from the plot slope of q_t vs. $t^{0.5}$ [20].

The contact time was an important factor affecting the detection limit and the sensitivity. The contact time was investigated in 10 mg L^{-1} BUT in the range of 1–120 min. The BUT separation percentage increased with time to the maximum value of 91% after 45 min.

A significant decrease of the concentration of the BUT solution occurred in the first 15 min, and then this trend became slow until equilibrium was reached. An agitation time of 45 min was selected for the subsequent adsorption. From the R^2 values in Table 1, the adsorption data of BUT solution fit well with the pseudo-second-order kinetic equation compared with the pseudo-first–order kinetic equation.

3.4. Adsorption isotherm

In order to evaluate the adsorption isotherm, Langmuir and Freundlich's equations were used (Table 2). The Langmuir isotherm is based on the hypothesis that uptake occurs on a homogeneous surface by monolayer adsorption without interaction between the adsorbed materials, which can be expressed as follows:

Table 1
Kinetic parameters for the adsorption of BUT with GO/Fe_3O_4/TSP/Den

Model	Parameter	Concentration, 10 mg L^{-1}
Pseudo-first-order kinetic	k_1 (min^{-1})	0.05
	q_e calculated (mg g^{-1})	2.04
	R^2	0.83
Pseudo-second-order kinetic	k_{ad} (min^{-1})	0.04
	q_e calculated (mg g^{-1})	3.3
	R^2	0.99
Intraparticle diffusion	k_{i1} (mg/(g min$^{1/2}$)	0.79

$$\frac{C_e}{q_e} = \frac{1}{bq_m} + \frac{C_e}{q_m} \quad (5)$$

Here C_e (mg L^{-1}) is the equilibrium concentration of the BUT solution, q_e (mg g^{-1}) is the adsorption capacity at equilibrium, and q_m and b are the maximum adsorption capacity (mg g^{-1}) and the equilibrium adsorption constant (L mg^{-1}), respectively.

The Freundlich isotherm can be expressed in the linear form by the following equation:

$$\ln q_e = \ln k + \frac{1}{n}\ln C_e \quad (6)$$

Here, k (L mg^{-1}) and n are the Freundlich constants [25].

Temkin isotherm has one factor which shows the interaction between the adsorbent and the adsorbing particle quite clearly. This model was applied in a form represented by Eq. (7) as follows:

$$q_e = B\ln A + B\ln C_e \quad (7)$$

By plotting q_e against ln C_e gives the constants A and B, which are the Temkin isotherm constant (L mg^{-1}) and the Temkin constant related to the heat of adsorption (J mol^{-1}), respectively, is the gas constant (8.314 mol K^{-1}). B is also a Temkin isotherm constant, which is an indication of the heat of adsorption indicating a physical adsorption process.

The adsorption isotherm is important for determining the adsorption behavior of an adsorbent. The isotherm curves demonstrate the adsorption as a function of the equilibrium concentration of the BUT solution. All three models—Langmuir, Freundlich, and Temkin—are used to normalize the adsorption.

3.5. Amount of the adsorbent

To select the optimal amount of the adsorbent (GO/Fe_3O_4/TSP/Den) for adsorption of BUT, different quantities of GO/Fe_3O_4/TSP/Den were assayed in the range of 0.005–0.07 g. Fig. 11 shows the effect of adsorbent dose on the adsorption of BUT. However, the amount of BUT removal increased from 54.5% to 91.1% as the amount of adsorbent added was from 0.005 to 0.03 g. When "GO/Fe_3O_4/TSP/Den" dose was increased from 0.03 to 0.07 g, the amount of removal was significantly reduced. In fact, the removal percentage increased to 3 g L^{-1} of the adsorbent, and then there was no addition and adsorption was in equilibrium. It is related to restricting access to the active adsorption positions. Besides, high concentrations of adsorbents can lead to the accumulation of adsorbents in the adsorption system, which can decrease the specific surface area and adsorption capacity.

3.6. Effect of temperature

In the adsorbent designed for this paper, a TSP was applied. And, as shown in Figs. 12(a) and (b), at an ambient

Table 2
Isotherm parameters for the adsorption of BUT with GO/Fe_3O_4/TSP/Den

Model	Parameter	Parameter value
Langmuir	q_m (mg g^{-1})	6.4
	b (L mg^{-1})	0.15
	R^2	0.99
Freundlich	$1/n$	0.52
	b (L mg^{-1})	–0.03
	k (mg g^{-1})	0.97
	R^2	0.97
Temkin	A_T (L mg^{-1})	–0.39
	b_T	2,022.8
	B (J mol^{-1})	1.2
	R^2	0.98

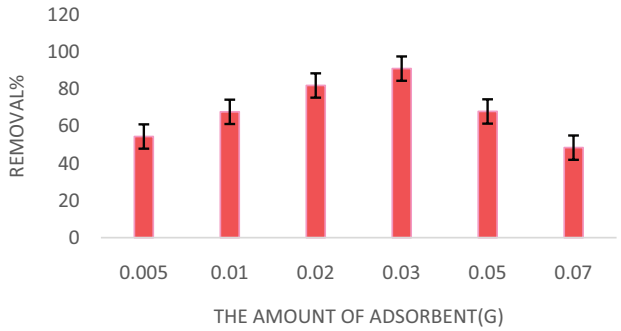

Fig. 11. Removal percentage of the amount of adsorbent.

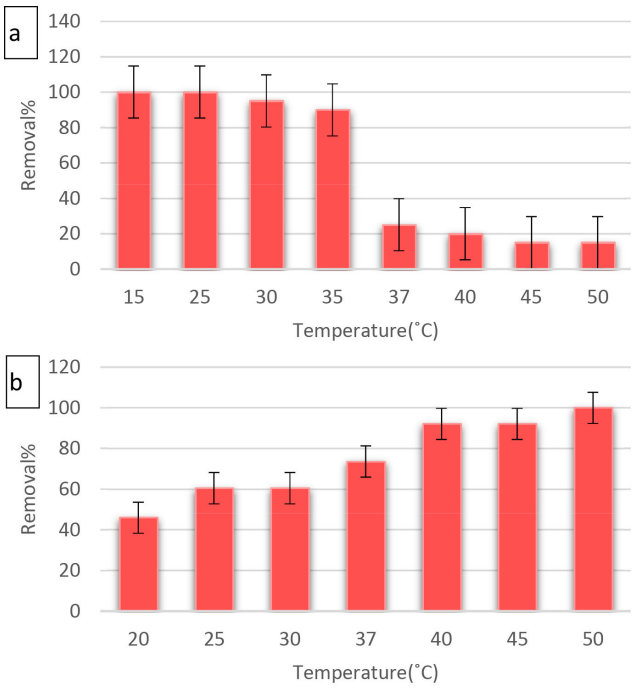

Fig. 12. Removal percentage of (a) absorption temperature and (b) desorption temperature.

temperature of 25°C, the adsorbent removed 100% of the pollutant. Moreover, at 37°C, the percentage of removal began to decrease, which indicated the susceptibility of the adsorbent to heat. Actually, when the temperature increased, TSP shrank and because of this phenomenon, the amount of pollution adsorption dropped. In the same way, the polymer was compressed and the rate of pollutants desorption expanded remarkably.

3.7. Adsorption thermodynamics

The thermodynamic criteria are evaluated through the computation of standard Gibbs free energy changes ($\Delta G°$), standard enthalpy changes ($\Delta H°$), and standard entropy changes ($\Delta S°$) by carrying out the adsorption experiments at three different temperatures to derive information about the energy changes associated with the adsorption process by using the following equations:

$$K_d = \frac{C_0 - C_e}{C_e}\frac{V}{m} \tag{8}$$

$$\ln K_d = \frac{\Delta S°}{R} - \frac{\Delta H°}{RT} \tag{9}$$

$$\Delta G° = \Delta H° - T\Delta S° \tag{10}$$

Here C_0 (mg L^{-1}) is the initial concentration of BUT solution, C_e (mg L^{-1}) is the equilibrium concentration, V (mL) is the volume of solution, m (g) is the dosage of sorbents, R is the universal gas constant (8.314 J mol^{-1} K^{-1}), and T (K) is the absolute temperature.

The values of $\Delta H°$ and $\Delta S°$ were determined from the slope and the intercept of the plots of $\ln K_d$ vs. $1/T$. The $\Delta G°$ values were calculated by using E_q [25].

As shown in Table 3 and Fig. 13, $\Delta H°$ possesses a mean value of 1.83 kJ mol^{-1}. The adsorption is endothermic because of the positive value of $\Delta H°$, which is supported by the increase of BUT adsorption onto GO/Fe_3O_4/TSP/Den at a higher temperature. The positive value of $\Delta S°$ demonstrates the increasing randomness at the solid/solution interface during the adsorption process. The value of $\Delta G°$ varies from –8.5 to –9.01 kJ mol^{-1} with the temperature rising from 25°C to 40°C. The negative value of $\Delta G°$ indicates the spontaneity and feasibility of the adsorption of BUT on the adsorbent.

3.8. Reusability of "GO/Fe_3O_4/TSP/Den"

Reusability is the main factor for estimating the efficiency of a magnetic sorbent. In order to realize reusability of the "GO/Fe_3O_4/TSP/Den" sorbent, it was used 10 times to extract BUT. It was figured out by following the repeated cycles of adsorption test. The remaining adsorption capacity was determined by comparing it with the first run (adsorption capacity defined as 100%). It was found that after 10 cycles, the loss of adsorption was just 6.7%.

Table 3
Thermodynamic parameters for the adsorption of BUT on GO/Fe_3O_4/TSP/Den

$\Delta H°$ (kJ mol^{-1})	$\Delta S°$ (kJ mol^{-1} K)	$\Delta G°$ (kJ mol^{-1})		
		298 K	303 K	313 K
1.83	0.035	–8.50	–8.67	–9.02

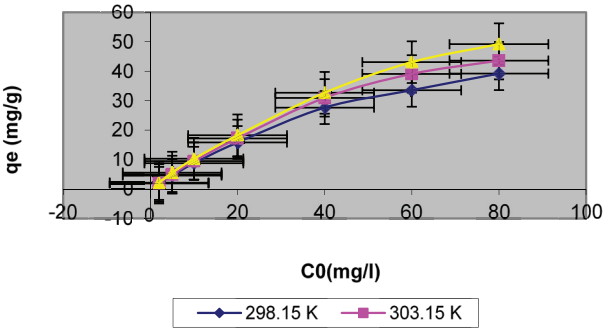

Fig. 13. Isotherm of BUT (2–80 mg L^{-1}) adsorption on GO/Fe_3O_4/TSP/Den (0.5 g L^{-1}) at different temperatures (298, 303, and 313 K).

3.9. Removal of BUT from a real water sample

In order to achieve the efficiency of the method in real matrices, it was applied for the analysis of BUT in an agricultural wastewater sample that was collected from the agricultural land upstream of the Doroudzan Dam. The prepared sample under the conditions mentioned in 2–10 mg/L was given to HPLC. It was found that the removal of BUT from a real water sample, notwithstanding the presence of some fertilizers and other toxins, was about 86.3%. The standard deviation was equal to 6.06%. The result confirmed the existence of BUT in the agricultural wastewater sample.

4. Conclusions

In summary, a magnetic nanocomposite of "GO/Fe_3O_4/TSP/Den" was successfully synthesized and used as an effective adsorbent for the removal of herbicide pollutants from agricultural wastewater. A new strategy for the modification of magnetic GO was dendrimerization. This large-scale method can be undertaken easily. While it is environmentally friendly, it is also cost-effective and saves energy. "GO/Fe_3O_4/TSP/Den" composites can efficiently remove concentrations of BUT from aqueous solutions and can also be easily separated from aqueous solution by a strong magnet. In our work, GO/Fe_3O_4/TSP/Den exhibited strong adsorption and high efficiency. Our adsorbent could successfully remove herbicides, especially BUT, in pH = 5, with the initial BUT concentration of 10 mg L^{-1}, 3 g L^{-1} of adsorbent, and at 25°C at 45 min. The adsorption followed the pseudo-second-order kinetics. The equilibrium data were suitably compatible with the Langmuir isotherm model. Furthermore, the negative value of $\Delta G°$ indicated the spontaneity and feasibility of the adsorption of BUT on the adsorbent. In conclusion, these composites have great potential applications for the removal of herbicides from polluted water.

References

[1] S. Becken, Water equity—contrasting tourism water use with that of the local community, Water Resour. Ind., 7–8 (2014) 9–22.
[2] B. Moss, Water pollution by agriculture, Philos. Trans. R. Soc. London, Ser. B, 363 (2008) 659–666.
[3] S. Mukhopadhyay, Nanotechnology in agriculture: prospects and constraints, Nanotechnol. Sci. App., 7 (2014) 63–71.
[4] Y. Pico, G. Font, J.C. Molto, J. Manes, Pesticides (New Generation) and Related Compounds, Encyclopedia of Analytical Chemistry, John Wiley & Sons, Ltd., 2002.
[5] Md. Shahidul Islam, M. Tanaka, Impact of pollution on coastal and marine ecosystems including coastal and marine fisheries and approach for management: a review and synthesis, Mar. Pollut. Bull. 48 (2004) 624–649.
[6] V. Singh, D. Joung, L. Zhai, S. Das, S. Khondaker, S. Seal, Graphene based materials: past, present and future, Prog. Mater. Sci., 56 (2011) 1178–1271.
[7] T. Kuila, S. Bose, A. Kumar Mishar, P. Khanra, N.H. Kim, J.H. Lee, Chemical functionalization of graphene and its applications, Prog. Mater. Sci., 57 (2012) 1061–1105.
[8] T. Kuila, S. Bose, A. Kumar Mishar, P. Khanra, N.H. Kim, J.H. Lee, Recent advances in graphene based polymer composites, Prog. Polym. Sci., 35 (2010) 1350–1375.
[9] D. Chen, H. Feng, J. Li, Graphene Oxide: Preparation, Functionalization, and Electrochemical Applications, Chem. Rev., 112 (2012) 6027–6053.
[10] A. Dimiev, L. Alemany, J. Tour, Graphene oxide. Origin of acidity, its instability in water, and a new dynamic structural model, ACS Nano, 7 (2013) 576–588.
[11] V. Georgakilas, M. Otyepka, A.B. Bourlinos, V. Chandra, N. Kim, K.C. Kemp, P. Hobza, R. Zboril, K.S. Kim, Functionalization of graphene: covalent and non-covalent approaches, derivatives and applications, Chem. Rev., 112, (2012) 6156–6214.
[12] N. Mahmoodi, M. Arami, N. Yousefi Limaee, K. Gharanjig, F. Nourmohamadian, Nanophotocatalysis using immobilized titanium dioxide nanoparticle: degradation and mineralization of water containing organic pollutant: a case study of Butachlor, Mater. Res. Bull. 42 (2007) 797–806.
[13] E. Roy, S. Patra, D. Kumar, R. Madhuri, P. Sharma, Multifunctional magnetic reduced graphene oxide dendrites: synthesis, characterization and their applications, Biosens. Bioelectron. 68 (2015) 726–735.
[14] N. Zubir, Ch. Yacou, J. Motuzas, X. Zhang, J. Diniz da Costa, Structural and functional investigation of graphene oxide–Fe_3O_4 nanocomposites for the heterogeneous Fenton-like reaction, Sci. Rep., 4 (2014) 4594.
[15] L. Guo, P. Ye, J. Wang, F. Fu, Z. Wu, Three-dimensional Fe_3O_4-graphene macroscopic composites for arsenic and arsenate removal, J. Hazard. Mater., 298 (2015) 28–35.
[16] Sh. Koushkbaghi, J. Jafari, M. Irani, M. Aliabadi, Fabrication of PET/PAN/GO/Fe_3O_4 nanofibrous membrane for the removal of Pb(II) and Cr(VI) ions, Chem. Eng. J. 301 (2016) 42–50.
[17] A. Naghizade, F. Mo'meni, Evaluation of graphene oxide nanoparticles efficacy in chromium and lead removal from aqueous solutions, J. Birjand Univ. Med. Sci., 22 (2012) 27–38 (in Persian).
[18] A. Mehdinia, N. Khodaee, A. Jabbari, Fabrication of graphene/Fe_3O_4@polythiophene nanocomposite and its application in the magnetic solid-phase extraction of polycyclic aromatic hydrocarbons from environmental water samples, Anal. Chim. Acta, 868 (2015) 1–9.
[19] H. He, Y. Li, T. Chen, X. Huang, Q. Guo, Sh. Li, Butachlor induces some physiological and biochemical changes in a rice field biofertilizer cyanobacterium, Pestic. Biochem. Physiol., 105 (2013) 224–230.
[20] H. Zhang, Ch. Zhang, G. Zeng, X. Gong, X. Ou, Sh. Huan, Easily separated silver nanoparticle-decorated magnetic graphene oxide: synthesis and high antibacterial activity, J. Colloid Interface Sci., 471 (2015) 94–102.
[21] O. Metin, S. Aydogan, K. Meral, A new route for the synthesis of graphene oxide–Fe_3O_4 (GO–Fe_3O_4) nanocomposites and their Schottky diode applications, J. Alloys Compd., 585 (2014) 681–688.
[22] E. Abbasi, S.F. Aval, A. Akbarzadeh, M. Milani, H. Tayefi Nasrabadi, S.W. Joo, Y. Hanifehpour, K. Nejati-Koshki, R, Pashaei-Asl, Dendrimers: synthesis, applications, and properties, Nanoscale Res. Lett., 9 (2014) 247
[23] X. Liu, Y. Tang, Sh. Luo, Y. Wanga, X. Zhan, Y. Che, Ch. Liu, Reduced graphene oxide and $CuInS_2$ co-decorated TiO_2 nanotube arrays for efficient removal of herbicide 2,4-dichlorophenoxyacetic acid from water, J. Photochem. Photobiol., A, 262 (2013) 22–27.
[24] Y. Tang, G. Zhang, Ch. Liu, Sh. Luo, X. Xu, L. Chen, B. Wang, Magnetic TiO_2-graphene composite as a high-performance and recyclable platform for efficient photocatalytic removal of herbicides from water, J. Hazard. Mater., 252–253 (2013) 115–122.
[25] M.M. Rahbar-Hashemi, M. Ashournia, M. Panahande, Removal of butachlor toxin polluted water using ozonation, a case study of groundwater resources in Guilan Province, J. Water Wastewater, 2 (2015) 114–123 (in Persian).
[26] X. Jin, K. Li, P. Ning, Sh. Bao, Removal of Cu(II) ions from aqueous solution by magnetic chitosan-tripolyphosphate modified silica-coated adsorbent: characterization and mechanisms, Water Air Soil Pollut., 8 (2017) 228–302.
[27] W. Wang, Y. Li, Q. Wu, Ch. Wang, Xi. Zang, Zh. Wang, Extraction of neonicotinoid insecticides from environmental water samples with magnetic graphene nanoparticles as adsorbent followed by the determination with HPLC, Anal. Methods, 4 (2012) 766.
[28] O. Saber, N.H. Mohammed, S.A. Arafat, Conversion of iron oxide nanosheets to advanced magnetic nanocomposites for oil spill removal, RSC Adv., 5 (2015) 72863–72871.